Structure and UV−Vis Spectrum of C_{60} Fullerene in Ethanol: A Sequential Molecular Dynamics/Quantum Mechanics Study

Thaciana Malaspina

Instituto de Química, Universidade de São Paulo, 05513-970 São Paulo, SP, Brazil

Eudes E. Fileti

Centro de Ciências Naturais e Humanas, Universidade Federal do ABC, 09210-270 Santo André, SP, Brazil

Roberto Rivelino*

Instituto de Física, Universidade Federal da Bahia, 40210-340 Salvador, BA, Brazil

Received: June 14, 2007; In Final Form: August 6, 2007

A molecular dynamics simulation combined with semiempirical quantum mechanics calculations has been performed to investigate the structure, dynamical, and electronic properties of pure C_{60} in liquid ethanol. The behavior of the fullerene alcoholic solution was obtained by using the NPT ensemble under ambient conditions, including one C_{60} fullerene immersed in 1000 ethanol molecules. Our analyzed center-of-mass pairwise radial distribution function indicated that, on average, there are 32, 72, 132, and 187 ethanol molecules around, respectively, the first, second, third, and fourth solvation shells of the C_{60} molecule. To investigate the UV−vis transition energies of C_{60} in the presence of ethanol, we have considered constituents of the time uncorrelated supramolecular structures of the first solvation shell, i.e., clusters of C_{60}@$\{EtOH\}_{32}$ types. The semiempirical calculations were performed at the intermediate neglect of differential overlap level with configuration interaction singles (INDO/CIS). Our results have pointed out that the characteristic C_{60} UV−vis absorbance peaks are slightly shifted to longer wavelengths, as compared to the isolated molecule. These findings are in connection with the weak donor−acceptor character of the interactions involving electron lone pairs of oxygen atoms on the solvent and the fullerene surface.

1. Introduction

Studies on the solubility of pure fullerenes in different solvents have been a task of great significance for understanding the interactions between these carbonaceous nanostructures with other molecules.[1−5] Moreover, the solvent plays a key role in investigations of the unique structural and chemical properties of fullerenes, as well as in the synthetic reactions that functionalize these species.[6−8] Because of these characteristic features, the solubility of fullerenes is also of interest in both applied and fundamental science. Among the main applications involving these carbon cages, biological use has attracted attention for obtaining soluble forms of C_{60} fullerene.[9−13] It is well-known that pristine fullerenes are poorly soluble in solvents that organize themselves through polar or H-bond interactions.[2,3] Specifically, the dissolution of a large nonpolar system like C_{60} implies the disruption of many intermolecular interactions in the solvent structure, without forming new ones with the fullerene surface.

On the other hand, the recent possibility of obtaining water-soluble forms of pure fullerenes[14,15] has permitted a deeper investigation of their interactions with other polar solvents. For instance, by means of an effective intermolecular potential framework, it has been demonstrated that the C_{60}−water interactions are dominated by relatively strong van der Waals attraction.[16] In this sense, molecular dynamics (MD) simulations have successfully been used to describe the solvent-induced repulsion of fullerenes in water[16,17] and the dynamics of hydration around C_{60}.[18] Also, by utilizing Monte Carlo simulations (MC), we have found that dispersion interactions, supplied by a realistic Lennard-Jones (LJ) potential,[19] lead to the formation of highly hydrated structures of fullerene in aqueous medium. Of course, the solubility of large nonpolar solutes also depends on their structural properties and the thermodynamic conditions.[11,20] Thus, the impact of finite temperature in the system is very important to assess the strength of solute−solvent interactions. These aspects have motivated our studies on solvated fullerenes under ambient conditions.[19,21]

In the present study, we have used fully atomistic MD simulations to generate suitable structures of solutions at room temperature and atmospheric pressure of C_{60} in ethanol, which is both a polar and H-bonding solvent. We also chose ethanol because it has recently been employed in preparing stable aqueous suspensions of colloidal C_{60} free of toxic organic solvents[11] via solvent exchange. Hence, we have explored the possibility of understanding the fullerene alcoholic solution by surveying the screening of the medium on the electronic structure of the solvated solute by ethanol, i.e., C_{60}@$\{EtOH\}_n$. To obtain the electronic properties of the solvated fullerene, after obtaining the dynamic properties, only time uncorrelated structures were selected to be used as input in the quantum mechanics (QM) calculations. These were performed at the semiempirical intermediate neglect of differential overlap level with singles configuration interaction (INDO/CIS). Along with the above methods, we have used a sequential procedure,[19,21−24]

* Corresponding author. Fax: +55-71-32836606. E-mail: rivelino@ufba.br.

10.1021/jp0746244 CCC: $37.00
Published on Web 09/25/2007

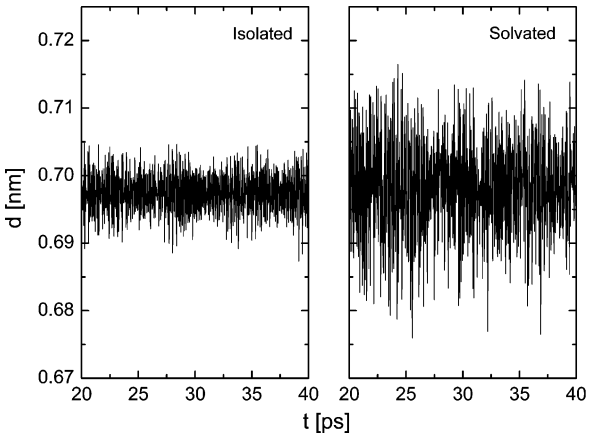

Figure 1. Diameter oscillation of the fullerene molecule during MD simulations: isolated (left) and solvated in ethanol (right).

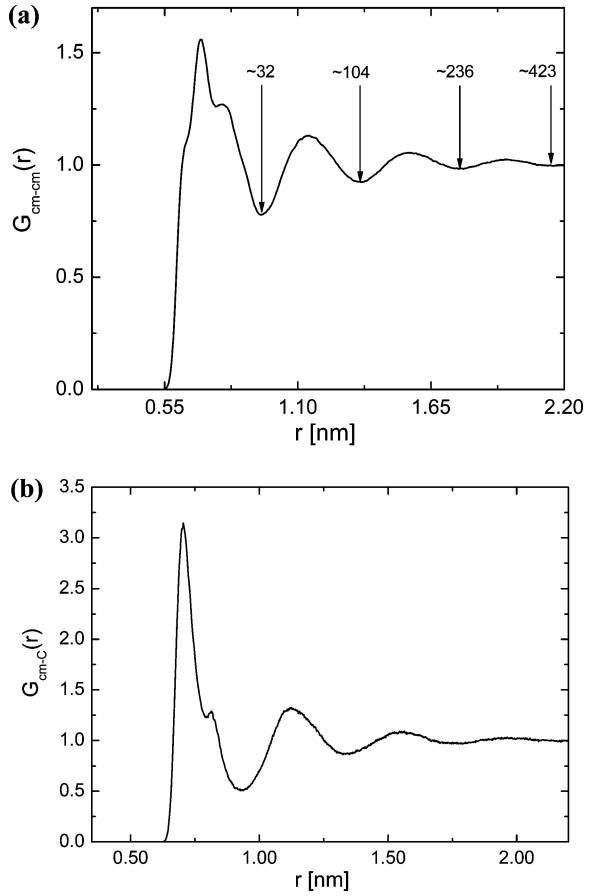

Figure 2. Radial distribution functions between C_{60} and ethanol. (a) In the center-of-mass−center-of-mass RDF, the number of ethanol molecules around the solute is obtained by spherical integration of $G_{cm-cm}(r)$. (b) Profile of the RDF between the center-of-mass of C_{60} and the carbon atoms on ethanol.

denoted here as MD/QM, to investigate the structure, dynamics, and UV−vis spectrum of a fullerene alcoholic solution.

2. Computational Details

Molecular Dynamics Simulations. Atomistic MD simulations using the isobaric−isothermal (NPT) ensemble were performed at 298 K and atmospheric pressure on a solution of one C_{60} fullerene in 1000 ethanol molecules, for which we have employed the all-atom optimized potential functions for liquid simulations (OPLS/AA) developed by Jorgensen.[25] This potential is harmonic flexible for bond-stretching and -bending and includes internal rotations of the ethanol molecule. By using the OPLS model, the conformational equilibrium of ethanol around fullerene has also been considered during the simulation. Additionally, this model fairly reproduces the dielectric properties of liquid ethanol in comparison with the polarizable force field proposed by Noskov et al.[26]

For the C_{60} molecule, we have adopted a 60-site model,[16,17,19] where each carbon atom was modeled as an uncharged LJ particle with a collision diameter $\sigma_C = 0.350$ nm and a potential well depth $\epsilon_C = 0.318$ kJ mol^{-1}. Two MD simulations have been performed: one using a rigid C_{60} molecule, within a geometry obtained at B3LYP/6-311+G(d,p),[27,28] and other considering the motions for bonds and angles of C_{60}. In this last case, the CC bond lengths and CCC bond angles were mimicked by harmonic potentials with spring constants obtained from the OPLS/AA force field mentioned previously.[25]

The solute−solvent interactions were only expressed as a LJ potential, whereas the solvent−solvent interactions are calculated by adding the Coulomb term, i.e.,

$$\Delta u_{ab} = \sum_{i}^{\text{on a}} \sum_{j}^{\text{on b}} \left\{ 4\epsilon_{ij} \left[\left(\frac{\sigma_{ij}}{r_{ij}} \right)^{12} - \left(\frac{\sigma_{ij}}{r_{ij}} \right)^{6} \right] + \frac{q_i q_j}{r_{ij}} \right\} \qquad (1)$$

In eq 1, Δu_{ab} is the interaction energy between molecules a and b, and the parameters ϵ_{ij} and σ_{ij} are obtained using the standard Lorentz−Berthelot combination rules.[29] The MD simulation has been carried out using the GROMACS program.[30−32] These were performed in cubic cells with periodic boundary condition employing the minimum image convention.[30]

The properties were calculated by considering a time-step of 2 fs with data collected every 0.02 ps. The cubic cells were equilibrated for 250 ps in a NPT ensemble at 1 atm, giving an average density of 804 kg m^{-3}. After the equilibration process, we have performed a running length of 800 ps. The system was kept at the appropriate temperature and pressure via Berendsen[33] and Parrinello−Rahman[34] schemes, with a constant coupling of 0.1 and 1.0, respectively. All bond lengths are constrained via the LINCS algorithm.[35] A cutoff distance of 1.0 nm for LJ interaction was employed, whereas the Coulomb interactions were treated by using the PME algorithm.[36]

The Sequential MD/QM Scheme. After performing the MD simulations, the next step was to generate the appropriate configurations of the fullerene alcoholic solution to submit as input for the QM calculations. Our procedure consisted of reducing thousands to hundreds of configurations[21−24] of the system without damaging the time averages (see ref 19 for details). In this case, only configurations separated by 10 ps were selected. This is enough of a time interval such that two successive configurations should be structurally uncorrelated. By using this scheme, we sampled 160 configurations for the QM supramolecular calculations, which were carried out at the semiempirical INDO/CIS level[37] for the first C_{60} solvation shell. All valence electron were included in the wave function, which is totally antisymmetric and delocalized over the solvent, allowing the contribution of the solvent polarization and dispersion interaction between the two subsystems.[38] Another advantage of this level of calculation is that the CIS method satisfies the size-extensivity requirement in the supramolecular calculations.[39] These features are rather important for calculating the spectroscopic properties of chromophores in solvents.

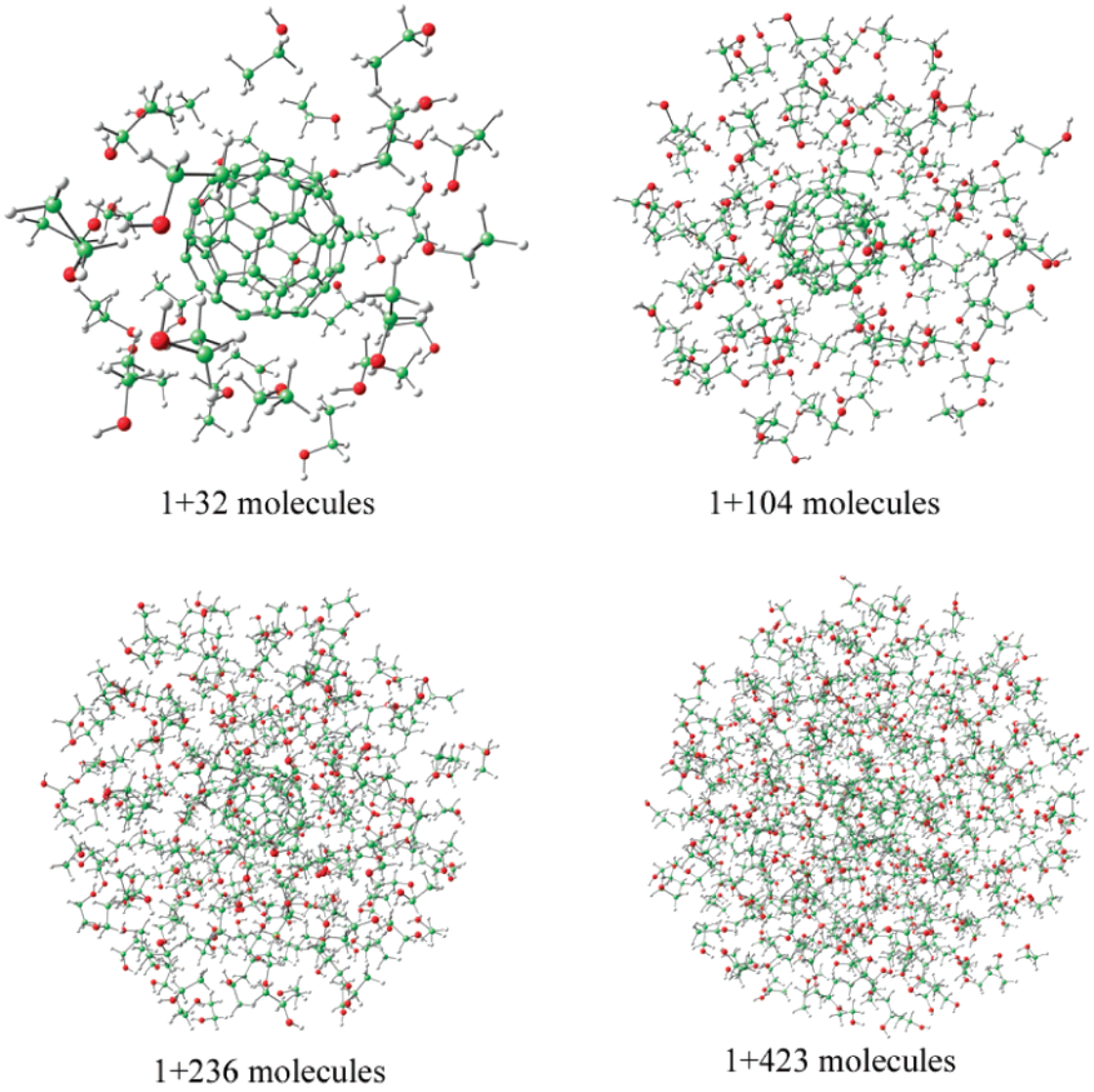

Figure 3. Illustration of the structures of the accumulated solvation shells around fullerene in ethanol, as calculated by the RDF spherical integration. Only one single structure of the alcoholic solution is represented.

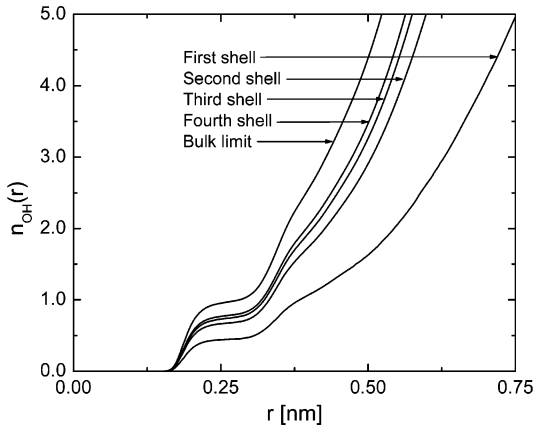

Figure 4. Variation of the coordinate number function of the O−H pairs from the first solvation shell up to the bulk limit.

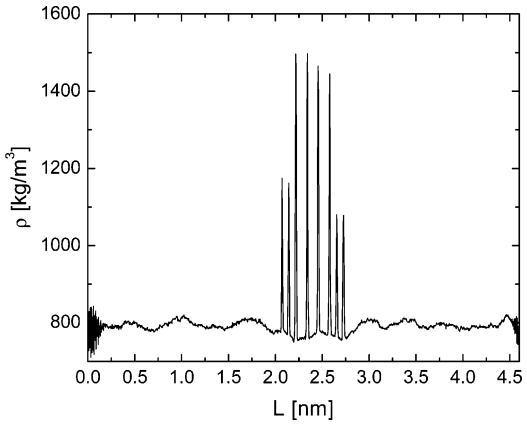

Figure 5. Partial density of the solution across the cell during the MD simulation as a function the cell size.

The sequential MD/QM procedure is very efficient and yields statistically converged results in such a way that the average transition energies can be written as

$$\langle \Delta E \rangle = \left(\frac{1}{L}\right)\sum_{i=1}^{L} \Delta E_i \qquad (2)$$

Therefore, the solvatochromic shifts were evaluated by subtracting the calculated transition energy of the isolated C_{60} molecule from the average transition energy of the supramolecular cluster given by eq 2, in which L refers to the number of MD configurations considered in the average. Both the ground and first excited electronic states of the isolated and solvated fullerene were calculated using the INDO/CIS, as implemented

in the ZINDO program.[40] As is well-known, INDO/CIS often produces accurately the type of low-lying excited states of molecular systems, which are dominated by single excitations.[39] A similar procedure[19] has yielded a very good agreement with the experimental UV−vis spectroscopic data for a fullerene aqueous solution.[15] Our calculations involving average electronic properties of uncorrelated supramolecular structures of $C_{60}@\{EtOH\}_n$ types give the picture of the fullerene alcoholic solution.

3. Results and Discussion

Structural Analysis. Figure 1 shows the diameter changes of the C_{60} molecule during the MD simulations in a vacuum (left side) and in ethanol solution (right side). The calculated average diameters in both conditions presented practically the same value, i.e., 0.697 nm, although the calculated standard deviation was smaller in the isolated system (0.002 nm) than in ethanol solution (0.009 nm). This result only indicates that in the solution C_{60} has larger amplitude of the breathing mode than in the gas phase, which is in agreement with the attractive van der Waals interactions between C_{60} and the medium. Analyzing both the rigid and flexible models of C_{60} in ethanol, we can see that only the diameter has presented a noticeable variation, while all other properties presented a very similar behavior in the MD simulations. Thus, thereafter, our calculated properties for the C_{60} in ethanol solution will be referred to the simulation using a rigid solute.

We display in Figure 2 the calculated radial distribution functions (RDF's) between C_{60} and ethanol. As can be seen in Figure 2a, four solvation shells are well-defined in this simulation. The first peak, starting at 0.70 nm and ending at the minimum value of 0.95 nm, corresponds to the first solvation shell with 32 ethanol molecules on average around C_{60}. The shoulder observed after the first peak is attributed to the methyl group in ethanol and can be clearly observed in the RDF between C_{60} and the carbon atoms on ethanol displayed in Figure 2b. The next peaks in Figure 2a appear at 1.14 nm (second shell), 1.56 nm (third shell), and 1.96 nm (fourth shell) with their respective minima at 1.36, 1.77, and 2.14 nm. The calculated average numbers of molecules in each of these shells are 72, 132, and 187, respectively. The accumulated number of molecules around the fullerene surface is illustrated in Figure 3, for one single structure extracted from the MD simulation.

An important feature analyzed here was the modification of the solvent structure around of the solute molecule. The first analysis is related to the reduction of H-bonds formed near the C_{60} surface. In pure liquid ethanol, the number of H-bonds is expected to be one per proton donor or two per oxygen acceptor.[41,42] In our investigation this number increased from the C_{60} surface, converging to the value of liquid ethanol in the bulk limit. Indeed, the increase of H-bonds can be observed from the n_{OH} coordinate number function for the O−H pairs displayed in Figure 4. This function was obtained by integration of the corresponding RDF. We notice that the n_{OH} converges to unity with the increase of the number of solvation shells. Other interesting analysis that pointed out modifications in the structure of the diluted solution of C_{60} in ethanol was obtained from the partial density across the cell. The profile of this property is shown in Figure 5, exhibiting a very appreciable change in the range between 2.0 and 2.7 nm, with peaks reaching up to 1500 kg m^{-3} near the C_{60} surface. Beyond this range, the density was estimated as being 800 kg m^{-3}.

UV−Vis Spectrum. For the calculations of the excitation energies of C_{60} in ethanol solution, at the INDO/CIS approximation, we have considered ca. 160 uncorrelated configurations of $C_{60}@\{EtOH\}_n$ types, obtained from the MD simulation. This means that the average values of the UV−vis transition energies were calculated over supramolecular clusters containing one fullerene molecule along with 32 ethanol molecules, which represent the first solvation shell of the system. The solvatochromic shift was evaluated by subtracting the calculated transition energy of the isolated C_{60} molecule from the average transition energy of all uncorrelated clusters using eq 2. As discussed above, the semiempirical INDO/CIS approach has been a very successful method for obtaining spectroscopic shifts in both polar and nonpolar solutes and solvents.[19,43,44]

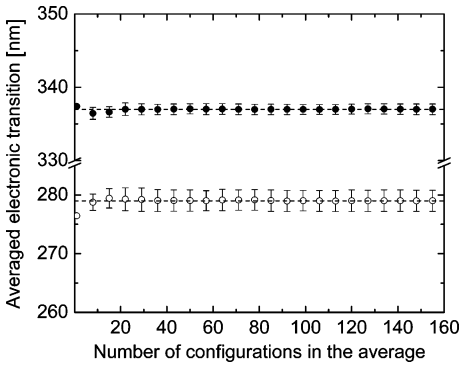

Figure 6. Convergence of the calculated transition energies in the absorption spectra of the solvated C_{60} under ambient conditions. Only the first solvation shell was taken into account in the calculations.

Our results have shown that the characteristic C_{60} UV−vis transition energies were slightly shifted to longer wavelengths, as compared to the isolated molecule. For instance, we have calculated average values of 279 ± 2 and 337 ± 1 nm for the solvated system, whereas our calculated values for the isolated fullerene were 266 and 331 nm. These values agree well with the UV−vis absorption spectra of C_{60} fullerene in toluene (269 and 335 nm)[15] and *n*-hexane (270 and 329 nm).[45] In comparison with other theoretical approaches, for instance TDDFT, the excited energies have been calculated systematically lower than experimental results for this system.[46] Furthermore, our results are in agreement with the expected formation of weakly bound complexes between C_{60} and electron-donor solvents like water.[8,14,15,45]

Figure 6 shows the convergence of two averaged electronic transitions of the solvated fullerene in ethanol. The calculated values converged rapid and systematically with the number of uncorrelated configurations considered in the averages. This indicates that the sampling was efficient for calculating the excitation energies of C_{60} in the presence of ethanol. These transitions presented a similar behavior to those observed in the experimental UV−vis absorption spectra of aqueous solutions, exhibiting peaks at 265 and 345 nm.[15,45] Indeed, it is well-known that the intermolecular interaction between C_{60} and electron-donor solvents is dominated by dispersion interactions, which are responsible for long-wavelength shifts in the optical spectra of fullerene, as compared to its isolated form. Thus, from the theoretical point of view, it is very important to take dispersion into account in the calculations. Also, we should emphasize that the calculated absorption spectra of $C_{60}@\{EtOH\}_{32}$ seems to be consistent to explain the UV−vis spectra of the whole fullerene ethanol solution. As in aqueous medium, these interactions between fullerene and the ethanol molecules should not change significantly the electronic struc-

ture of the solute. Thus, the optical spectra of noninteracting C_{60} molecules must differ slightly from those of their solvated states.

4. Summary and Conclusions

In this work, the structural features of C_{60} fullerene in ethanol solution were investigated from MD simulation at room temperature and atmospheric pressure. Our analysis has predicted the existence of spherically symmetric solvated clusters containing supramolecular complexes of $C_{60}@\{EtOH\}_n$ types. These are mainly stabilized by dispersion interaction between C_{60} and ethanol and also by reordering of hydrogen-bonded ethanol molecules around C_{60}. The ground and first excited energies of C_{60}, including its first solvation shell, were calculated using the INDO/CIS approximation. To perform these calculations, an efficient sequential MD/QM methodology has been employed. In this sense, we have successfully calculated the UV−vis spectral shifts of the fullerene alcoholic solution considering only the screening of 32 ethanol molecules around C_{60}. For instance, the largest calculated red-shift in $C_{60}@\{EtOH\}_{32}$ was the small amount of 13 ± 2 nm for the more intense transition. This seems to be very similar to the corresponding red-shift measured in aqueous solutions.

The QM calculations involved 160 uncorrelated configurations of clusters $C_{60}@\{EtOH\}_{32}$. Each calculation started with an appropriate antisymmetric wave function of 880 valence electrons. The transition energies were calculated via singly excited configuration interaction. Then, we have obtained converged averages of the transition energies for the solvated state of C_{60} at 279 ± 2 and 337 ± 1 nm. Actually, these values are in the expected range of both experimental and theoretical calculations for C_{60} in polar solvents. Our results have shown that in ethanol the characteristic C_{60} UV−vis absorbance peaks are slightly shifted to longer wavelengths. Therefore, these findings are in connection with the weak donor−acceptor character of the interactions involving electron lone pairs of oxygen atoms on alcohols and the fullerene surface. Moreover, our results showed that including only the first hydration shell around C_{60} was enough to analyze the spectral properties of the solvated fullerene. Finally, by using this theoretical methodology we expect to contribute to the elucidation of both the structure and electronic properties of solvated fullerenes in polar media.

Acknowledgment. This work has been partially supported by the Brazilian agencies FAPESP, Fapesb, and CNPq. E.E.F. is grateful to Luciano T. Costa and Paul van Maaren for helpful discussions.

References and Notes

(1) Marcus, Y.; Smith, A. L.; Korobov, M. V.; Mirakyan, A. L.; Avramenko, N. V.; Stukalin, E. B. *J. Phys. Chem. B* **2001**, *105*, 2499.

(2) Ruoff, R. S.; Tse, D. S.; Malhotra, R.; Lorents, D. C. *J. Phys. Chem.* **1993**, *97*, 3379.

(3) Ruoff, R. S.; Malhotra, R.; Huestis, D. L.; Tse, D. S.; Lorents, D. C. *Nature* **1993**, *362*, 140.

(4) Sawamura, S.; FujitaN. *Carbon* **2007**, *45*, 965.

(5) Avramenko, N. V.; Korobov, M. V.; Parfenova, A. M.; Dorozhko, P. A.; Kiseleva, N. A.; Dolgov, P. V. *J. Therm. Anal. Calorim.* **2006**, *84*, 259.

(6) Nakamura, E.; Isobe, H. *Acc. Chem. Res.* **2003**, *36*, 807.

(7) Kim, H.; Bedrov, D.; Smith, G. D.; Shenogin, S.; Keblinski, P. *Phys. Rev. B* **2005**, *72*, 085454.

(8) Prylutskyy, Y. I.; Durov, S. S.; Bulavin, L. A.; Adamenko, II; Moroz, K. O.; Geru, II; et al. *Int. J. Thermophys.* **2001**, *22*, 943.

(9) Sayes, C. M.; Fortner, J. D.; Guo, W.; Lyon, D.; Boyd, A. M.; Ausman, K. D.; Tao, Y. J.; Sitharaman, B.; Wilson, L. J.; Hughes, J. B.; West, J. L.; Colvin, V. L. *Nano Lett.* **2004**, *4*, 1881.

(10) Gharbi, N.; Pressac, M.; Hadchouel, M.; Szwarc, H.; Wilson, S. R.; Moussa, F. *Nano Lett.* **2005**, *5*, 2578.

(11) Dhawan, A.; Taurozzi, J. S.; Pandey, A. K.; Shan, W.; Miller, S. M.; Hashsham, S. A.; Tarabara, V. V. *Environ. Sci. Technol.* **2006**, *40*, 7394.

(12) Fortner, J. D.; Lyon, D. Y.; Sayes, C. M.; Boyd, A. M.; Falkner, J. C.; Hotze, E. M.; Alemany, L. B.; Tao, Y. J.; Guo, W.; Ausman, K. D.; Colvin, V. L.; Hughes, J. B. *Environ. Sci. Technol.* **2005**, *39*, 4307.

(13) Deguchi, S.; Yamazaki, T.; Mukai, S.; Usami, R.; Horikoshi, K. *Chem. Res. Toxicol.* **2007**, *20*, 854.

(14) Andrievsky, G. V.; Klochkov, V. K.; Kariakina, E. L.; Mchedlov-Petrossyan, N. O. *Chem. Phys. Lett.* **1999**, *300*, 392.

(15) Scharff, P.; Risch, K.; Carta-Abelman, L.; Dmytuk, I. M.; Bilyi, M. M.; Golub, O. A.; et al. *Carbon* **2004**, *42*, 1203.

(16) (a) Li, L. W.; Bedrov, D.; Smith, G. D. *J. Chem. Phys.* **2005**, *123*, 204504. (b) Li, L. W.; Bedrov, D.; Smith, G. D. *Phys. Rev. E* **2005**, *71*, 011502.

(17) Werder, T.; Walther, J. H.; Jaffe, R. L.; Halicioglu, T.; Koumoutsakos, P. *J. Phys. Chem. B* **2003**, *107*, 1345.

(18) (a) Choudhury, N. *J. Chem. Phys.* **2006**, *125*, 034502. (b) Choudhury, N. *J. Phys. Chem. C* **2007**, *111*, 2565.

(19) Rivelino, R.; Maniero, A. M.; Prudente, F. V.; Costa, L. S. *Carbon* **2006**, *44*, 2925.

(20) Ashbaugh, H. S.; Paulaitis, M. E. *J. Am. Chem. Soc.* **2001**, *123*, 10721.

(21) Rivelino, R.; de Brito Mota, F. *Nano. Lett.* **2007**, *7*, 1526.

(22) (a) Rivelino, R.; Cabral, B. J. C.; Coutinho, K.; Canuto, S. *Chem. Phys. Lett.* **2005**, *407*, 13. (b) Rivelino, R.; Coutinho, K.; Canuto, S. *J. Phys. Chem. B* **2002**, *106*, 12317.

(23) Malaspina, T.; Coutinho, K.; Canuto, S. *J. Chem. Phys.* **2002**, *117*, 1692.

(24) Fileti, E. E.; Malaspina, T.; Coutinho, K.; Canuto, S. *Phys. Rev. E* **2003**, *61*, 61504.

(25) Jorgensen, W. L. *J. Phys. Chem.* **1986**, *90*, 1276.

(26) Noskov, S. Y.; Lamoureux, G.; Roux, B. *J. Phys. Chem. B* **2005**, *109*, 6705.

(27) (a) Becke, A. D. *J. Chem. Phys.* **1993**, *98*, 5648. (b) Lee, C.; Yang, W.; Parr, R. G. *Phys. Rev. B* **1988**, *37*, 785.

(28) Schmidt, M. W.; Baldridge, K. K.; Boatz, J. A.; Elbert, S. T.; Gordon, M. S.; Jensen, J. H.; et al. *J. Comput. Chem.* **1993**, *14*, 1347.

(29) Allen, M. P.; Tildesley, D. J. *Computer Simulations of Liquids;* Clarendon Press: Oxford, 1987.

(30) Lindahl, E.; Hess, B.; van der Spoel, D. *J. Mol. Model.* **2001**, *7*, 306.

(31) Berendsen, H. J. C.; Vanderspoel, D.; Vandrunen, R. *Comput. Phys. Commun.* **1995**, *91*, 43.

(32) van der Spoel, D.; Lindahl, E.; Hess, B.; Groenhof, G.; Mark, A. E.; Berendsen, H. J. C. *J. Comput. Chem.* **2005**, *26*, 1701.

(33) Berendsen, H. J. C.; Postma, J. P. M.; van Gunsteren, W. F.; DiNola, A.; Haak, J. R. *J. Chem. Phys.* **1984**, *81*, 3684.

(34) Parrinello, M.; Rahman, A. *J. App. Phys.* **1981**, *52*, 7182.

(35) Hess, B.; Bekker, H.; Berendsen, H. J. C.; Fraaije, J. G. E. M. *J. Comput. Chem.* **1997**, *18*, 1463.

(36) Darden, T.; York, D.; Pedersen, L. *J. Chem. Phys.* **1993**, *98*, 10089.

(37) Ridley, J.; Zerner, M. *Theor. Chim. Acta* **1973**, *32*, 111.

(38) Canuto, S.; Coutinho, K.; Zerner, M. C. *J. Chem. Phys.* **2000**, *112*, 7293.

(39) (a) Zerner, M. C.; Lowe, G. H.; Kirchner, R. F.; Mueller-Westerhoff, U. T. *J. Am. Chem. Soc.* **1980**, *102*, 589. (b) Zerner, M. C. Semiempirical molecular orbital methods. In *Reviews of Computational Chemistry*, Lipkowitz, K. B., Boyd, D. B., Eds.; VCH: New York, 1990; vol 2, pp 313−365.

(40) Zerner, M. C. *ZINDO, a semi-empirical program package*. University of Florida, Gainesville, FL, 1996.

(41) Padro, J. A.; Saiz, L.; Guardia, E. *J. Mol. Struct.* **1997**, *416*, 243.

(42) Saiz, L.; Padro, J. A.; Guardia, E. *J. Phys. Chem. B* **1997**, *101*, 78.

(43) (a) Canuto, S.; Coutinho, K.; Trzesniak, D. *Adv. Quantum Chem.* **2002**, *41*, 161. (b) Coutinho, K.; Canuto, S. *J. Chem. Phys.* **2000**, *113*, 9132.

(44) Georg, H. C.; Coutinho, K.; Canuto, S. *J. Chem. Phys.* **2007**, *126*, 034507.

(45) Andrievsky, G. V.; Klochkov, V. K.; Bordyuh, A.; Dovbeshko, G. I. *Chem. Phys. Lett.* **2002**, *364*, 8.

(46) Bauernschmitt, R.; Ahlrichs, R.; Hennrich, F. H.; Kappes, M. M. *J. Am. Chem. Soc.* **1998**, *120*, 5052.